Nanoscale Advances

ROYAL SOCIETY OF CHEMISTRY

PAPER

View Article Online
View Journal | View Issue

Cite this: *Nanoscale Adv.*, 2023, **5**, 1397

Efficient red luminescence in Eu^{3+} doped CdSe/CdS all-inorganic quantum dots shows great potential for wLEDs†

Zhi Chen, *[ab] Yonggui Li[a] and Lixin Wu [b]

Complete inorganic quantum dots (QDs) CdSe/CdS:Eu^{3+} with full transmittance were proposed as red color converters for white light emitting diodes (wLEDs) using a facile one-step melt quenching method. TEM, XPS, and XRD were used to verify the successful nucleation of CdSe/CdS:Eu^{3+} QDs in silicate glass. The results indicated that the incorporation of Eu contributed to the nucleation of CdSe/CdS QDs in silicate glass, where the nucleation time of the CdSe/CdS:Eu^{3+} QDs rapidly decreased in 1 h compared with other inorganic QDs that took more than 15 h. CdSe/CdS:Eu^{3+} inorganic QDs exhibited bright and long-term stable red luminescence under both UV and blue light excitation; up to 53.5% quantum yield and 8.05 ms fluorescence lifetime were obtained by adjusting the Eu^{3+} concentration. Based on the luminescence performance and absorption spectra, a possible luminescence mechanism was proposed. Moreover, the application potential of the CdSe/CdS:Eu^{3+} QDs in wLEDs was studied by coupling the CdSe/CdS:Eu^{3+} QDs and commercial Intematix G2762 green phosphor on a InGaN blue LED chip. Warm white light (5217 K) with 89.5 CRI and 91.1 lm W^{-1} luminous efficacy could be achieved. Additionally, 91% of the NTSC color gamut was obtained, demonstrating the great potential of the CdSe/CdS:Eu^{3+} inorganic QDs as a color converter for wLEDs.

Received 4th November 2022
Accepted 25th January 2023

DOI: 10.1039/d2na00774f

rsc.li/nanoscale-advances

Introduction

White LED (wLED) is one of the most important optical devices in people's daily lives. To date, most commercial wLEDs have been obtained using an InGaN-based blue LED chip to excite commercial $Y_3Al_5O_{12}$:Ce^{3+} (YAG:Ce^{3+}; yellow) phosphor or $Lu_3Al_5O_{12}$:Ce^{3+} (LuAG:Ce^{3+}; green) and $CaAlSiN_3$:Eu^{2+} (CASN:Eu^{2+}; red) composite phosphors.[1,2] However, the absence of red components in the first white light scheme resulted in a low color rendering index (CRI) and cool white light. However, the low luminous efficiency and transparency of red phosphors used in the second white light scheme resulted in low luminous efficacy for the wLED.[3] In comparison with red phosphor, the red QD was regarded as the most potential luminescent material to replace red phosphor and as a color converter for wLED because of its high quantum efficiency, narrow full width at half maximum (FWHM), high fluorescence efficiency, and wide color gamut.[4–6] However, the disadvantages of agglomeration, weak thermal stability and atmospheric sensitivity of colloidal QDs (CQDs) should be addressed before their practical applications in wLEDs.[7] Recently, synthesizing all-inorganic QD was proposed to overcome the disadvantages of CQDs by encapsulating QDs in a silicate glass matrix because of non-reactivity, moisture and thermal resistance of inorganic glasses.[8,9] To date, various semiconductor and perovskite inorganic QDs have been successfully synthesized within a silicate glass matrix *via* a thermal nucleation and growth process using the melt-quenching method, which absolutely presents their promising characteristics and optical performance depending on the element composition, QD particle size, and structure.[10–12] $CsPbX_3$ (X = Cl/Br/I) halide perovskite QDs in glass are widely studied inorganic QDs because of their high quantum yield, narrow FWHM, and tunable emission.[13,14] However, the low quantum efficacy (<14%) and transmittance (<10%) of the red halide perovskite QD glass ($CsPbI_3$) limit its application potential in wLED although the halide perovskite QDs with full emission color from blue to red have been achieved by adjusting the ratio of halide elements.[15,16] Even though great endeavors have been made and reported, the quantum efficiency of red-emitting $CsPbI_3$ QDs could be partly improved by incorporating specific elements, such as fluorine and Eu^{3+}, into the QD glass matrix. Under the high temperature and poor transmittance of $CsPbI_3$ QD glass, the volatile characteristics of halide element I were also huge challenges for its practical application in optical devices.[17–19] Except for inorganic perovskite QDs, inorganic IIB-VIA group semiconductor QDs, such as PbS, PbSe, CdSe, CdS, and ZnS, have attracted considerable

[a]*Fujian Key Laboratory of Novel Functional Textile Fibers and Materials, Minjiang University, Fuzhou, 350108, China. E-mail: chenzhi@fjirsm.ac.cn*

[b]*Fujian Institute of Research on the Structure of Matter, Chinese Academy of Sciences, Fuzhou, 350002, China*

† Electronic supplementary information (ESI) available. See DOI: https://doi.org/10.1039/d2na00774f

attention in recent years.[20–23] The advantages of high transparency, a long fluorescence lifetime, and easy precipitation in the glass matrix also show great application potential in optical devices. However, similar to the red perovskite QDs, the IIB-VIA group red QDs show relatively low quantum efficiency, which hinders their feasibility as color converters for wLEDs. The preparation of novel red-emitting all-inorganic QDs with high quantum efficiency and transmittance is still an urgent task.

To address the low quantum efficiency of IIB-VIA group red emitting inorganic QDs, we proposed and designed a novel all-inorganic transparent CdSe/CdS:Eu^{3+} red-emitting QDs by doping rare earth Eu^{3+} ions into the crystalline of CdSe/CdS co-exited QDs based on the characteristic $^5D_0$–$^7F_2$ energy level transition of Eu^{3+} ions.[24–26] Compared with other inorganic QDs, this CdSe/CdS:Eu^{3+} inorganic QD shows full transmittance and bright red fluorescence with 53.5% of QY under excitation of blue light (465 nm) and significantly reduces the preparation time (more than 10 h saved). Therefore, the CdSe/CdS:Eu^{3+} inorganic QD shows great potential as a color converter for wLED.

Experimental

Preparation

$65SiO_2$–$25Na_2CO_3$–5BaO–5ZnO–10%H_3BO_3 (in mol%) glass system was selected as the QD glass matrix, and QD raw materials, which consisted of 0.65ZnS–0.85ZnSe–0.75CdO (in mol%), were mixed with the glass matrix materials and ground into powders for a certain time. Then, Eu_2O_3 was selected to provide Eu^{3+} and introduced into the QD crystalline based on the theoretical calculation and luminescence of the actual product. The CdSe/CdS:$x$$Eu^{3+}$ inorganic QDs were synthesized by a facile one-step melt-quenching method and by adjusting the mole concentration variation of Eu^{3+} ions from 0.08% to 0.8%. In detail, the mixed raw materials were melted in a muffle furnace at 1000 °C for 1 h under ambient atmosphere with a heating rate of 5 °C min^{-1}. Subsequently, the melts were removed immediately from the muffle furnace, promptly poured into a brass mold and annealed at 400 °C for 3 h to release thermal stress. Next, the CdSe/CdS:Eu^{3+} QD glasses were obtained when the temperature cooled to room temperature naturally (see Fig. S1†). Moreover, a blank sample (CdSe/CdS QDs without Eu^{3+} ion doping) was prepared using a similar method for comparison. Finally, the as-prepared CdSe/CdS:Eu^{3+} QDs blended with commercial green phosphor (Intematix G2762 CIE chromaticity coordinate $x = 0.25$, $y = 0.64$) were mounted on an InGaN blue LED chip (465 nm) to assemble the wLED to examine the color conversion (The specific preparation of the wLED was supplied in ESI material part 2.†).

Characterization

To confirm the growth of the CdSe/CdS:Eu^{3+} QDs in glass, X-ray diffraction (XRD, D8 Advance, Bruker, Germany) measurements were carried out with CuKα radiation operating at 40 kV and 30 mA in the range of 10–80° (2 theta) at a rate of 8° s^{-1}. Microstructure observations of CdSe/CdS:Eu^{3+} solid QDs were carried out using an FEI Tecnai G2 F20 TEM operated at 200 kV accelerating voltage. High-resolution TEM (HR-TEM) images were taken using an FEI aberration-corrected Titan-Cubed S-Twin transmission electron microscope operated on a HAADF mode. X-ray photoelectron spectroscopy (XPS) was carried out in a Thermo scientific 250Xi spectrometer equipped with a monochromatic Al Kα X-ray source ($h\nu = 1486.6$ eV) operated at 150 W. Photoluminescence (PL) spectra and fluorescence lifetime were recorded by applying a Hitachi F-7100 spectrophotometer equipped with continuous (450 W) xenon lamps. The quantum yield (QY) and CIE chromaticity coordinates were measured using an Edinburgh FLS 1000 spectrofluorometer. Specifically, the QY measurement should be taken in an integrating sphere and obtained by calculating the ratio of emitted photons to those absorbed by the QD samples. The absorption spectra were collected using a Lambda 950 UV-Vis spectrophotometer (PerkinElmer, USA). The optical properties of the QDs/phosphors converted wLEDs, including the color rendering index (CRI), correlated color temperature (CCT), electroluminescence (EL) spectra, and luminous efficacy (LE), were evaluated using a spectroradiometer system that consisted of an integrating sphere (PMS-50, Everfine, China) and a CCD spectrometer (CDS2100, Labsphere Inc., USA).

Results and discussion

Fig. 1a presents the TEM image of the CdSe/CdS:Eu^{3+} QDs samples; it can be observed that the QDs dispersed well in the inorganic glass matrix with an average diameter of 1.8 nm (Fig. S2†). The HR-TEM image of the QDs shown in Fig. 1b revealed that QDs possess interplanar distances of 0.373, 0.351, 0.358, and 0.316 nm, corresponding to the (100), (002), (100), and (101) lattice planes of CdSe and CdS.[27,28] Moreover, the XRD patterns were investigated to verify the successful synthesis of the inorganic CdSe/CdS:Eu^{3+} QDs in glass. As illustrated in Fig. 1c, although there is no sharp diffraction peak emerging due to the nano particle size of the inorganic QDs, part of the weak characteristic diffraction peaks can be observed compared with the XRD patterns of the blank samples without Eu ion doping (see Fig. S3†), which agrees with standard CdSe JCPDS#77-2307 and CdS JCPDS#77-2306. This verifies the formation of CdSe and CdS QDs and the contribution of Eu^{3+} ions to the nucleation and crystalline growth of CdSe and CdS QDs in the glass matrix. By continuously increasing the mole concentrations of Eu^{3+} ions to 0.8%, some of the characteristic diffraction peaks of the samples disappeared, and some new diffraction peaks appeared in the XRD patterns, indicating that the ordered crystal structure of the CdSe/CdS QDs may be destroyed by incorporating Eu ions. Except for CdSe and CdS, no characteristic diffraction peak of ZnSe of ZnSeS can be observed, implying that the element of Zn does not participate in the crystallization of the QDs in glass. This may be attributed to the short synthesis time of the QD glass. Notably, although the TEM images and XRD patterns showed the existence of CdSe and CdS QDs in glass, the structure of CdSe/CdS:Eu^{3+} QD could not be confirmed.

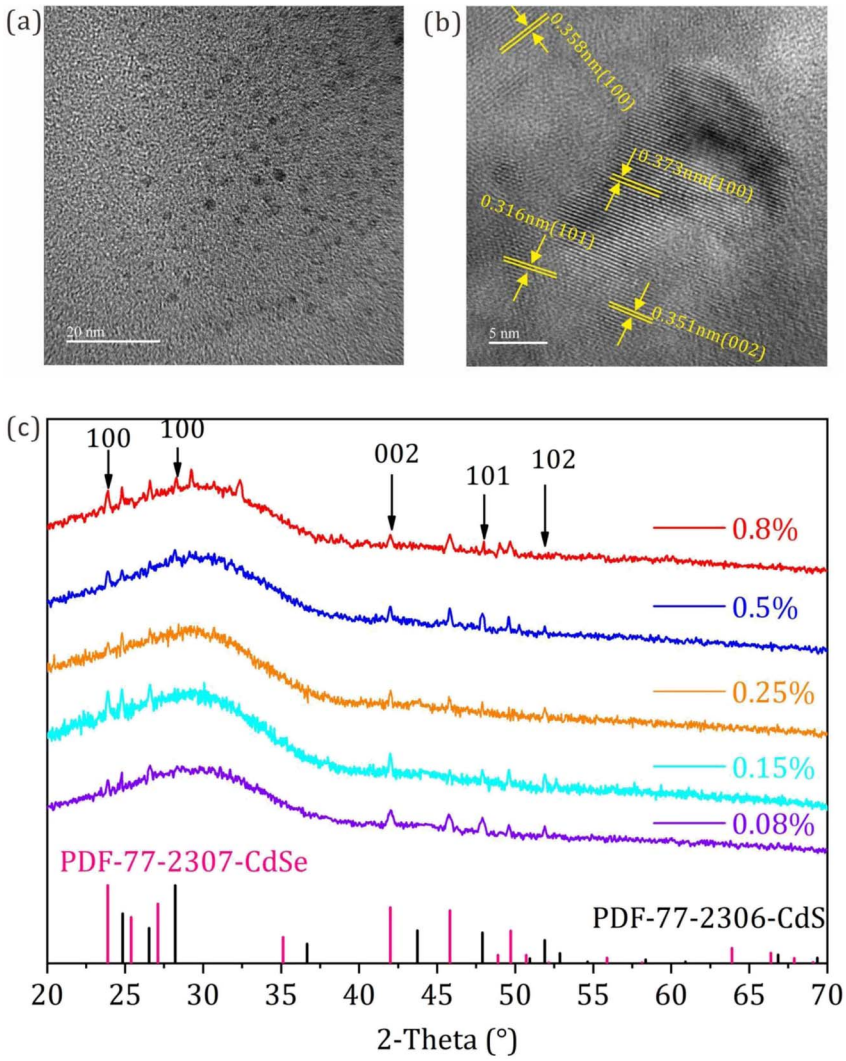

Fig. 1 (a) and (b) TEM and HR-TEM images; (c) XRD patterns of the CdSe/CdS:Eu^{3+} QDs with different Eu^{3+} concentrations of Eu^{3+} doping.

XPS comparative analyses of the inorganic CdSe/CdS:Eu^{3+} QDs are carried out to further confirm the incorporation of Eu^{3+} ions. Fig. 2a illustrates a full-scan spectrum for all elements in CdSe/CdS:Eu^{3+} QDs. The characteristic peaks of the main elements of Cd and Se can be clearly found, but the peaks of Eu and S are too weak to be discovered because of the low levels of these two elements in the QDs. Fig. 2b–e shows high-resolution XPS narrow-sweep spectra for the elements of Eu 3d, Cd 3d, Se 3d, and S 5p. The characteristic peaks at 1163 eV and 1134 eV binding energies, which were assigned to Eu $3d_{3/2}$ and Eu $3d_{5/2}$, further verified the fact that Eu^{3+} was successfully introduced into QDs. Cd 3d revealed two peaks with banding energies of 412 eV and 405.4 eV, which correspond to Cd $3d_{3/2}$ and Cd $3d_{5/2}$. In addition, the single peak at 63.2 eV binding energy originated from Se 3d, and the peak at 168.7 eV was assigned to S 2p. Comparing the XPS peak intensity and location of all the QD elements, the binding energies of all the QD element XPS spectra exhibited small variations, whereas the intensity of the Eu 3d peaks increased along with the Eu^{3+} ion concentration from 0.08% to 0.8%. The results confirmed the fact that Eu^{3+} ions entered the lattice of CdSe/CdS QDs and generated enhanced Eu–Cd–Se and Eu–Cd–S bonds with the increase of Eu^{3+} doping.

The PL excitation and emission spectra of the CdSe/CdS:Eu^{3+} inorganic QDs incorporated with different concentrations of Eu^{3+} ions are shown in Fig. 3a and b to explore their optical properties. In compassion with the excitation spectrum of the blank sample (Fig. S4a†), sharper excitation peaks that originated from Eu^{3+} ions emerged from 350 to 550 nm in the excitation spectra of CdSe/CdS:Eu^{3+} inorganic QDs. The highest excitation peaks at 393 nm and 465 nm implied that the CdSe/CdS:Eu^{3+} QDs could be best excited by both UV and visible light, especially blue light. The emission band under the excitation of 465 nm comprises a continuous broad band from 575 nm to 675 nm with multiple emission peaks at 580, 592, 612, and 656 nm, thereby verifying that the CdSe/CdS:Eu^{3+} QDs could be excited by blue light to emit red luminescence. Specifically, except for the peak of 580 nm belonging to the yellow emission

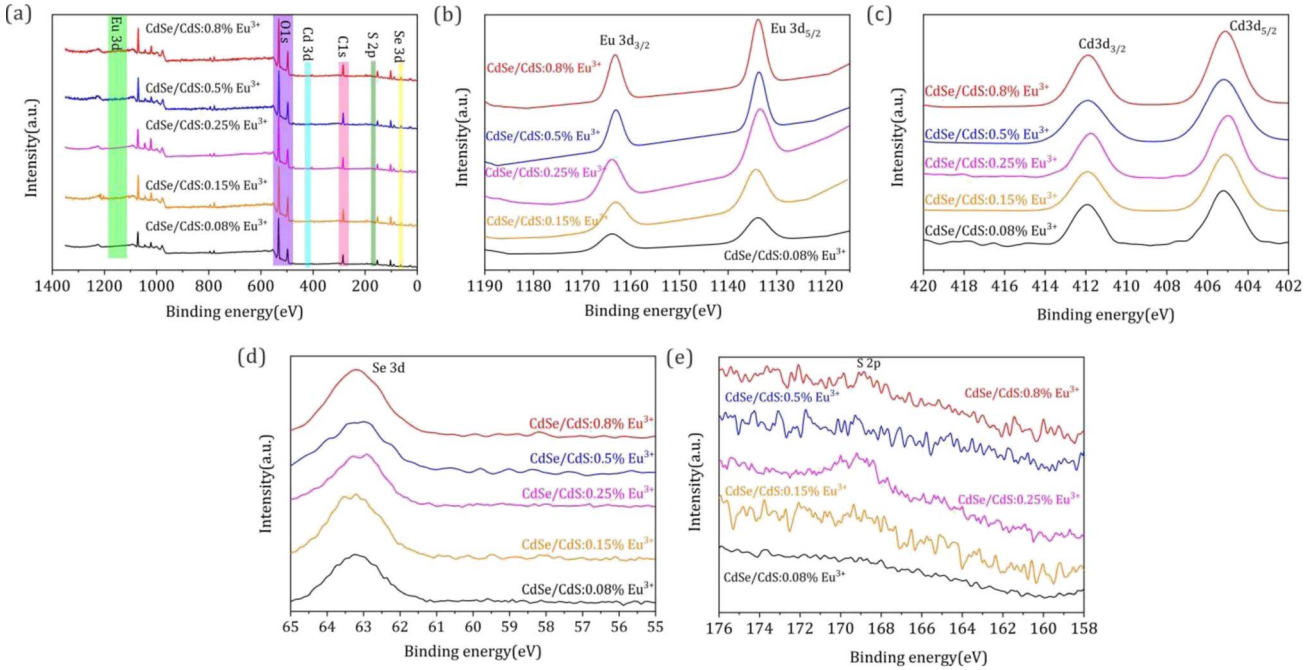

Fig. 2 (a) XPS survey spectra of CdSe/CdS:Eu^{3+} QDs with different Eu^{3+} concentrations. (b)–(e) The high-resolution XPS analysis corresponds to Eu 3d, Cd 3d, Se 3d, and S 2p, separately.

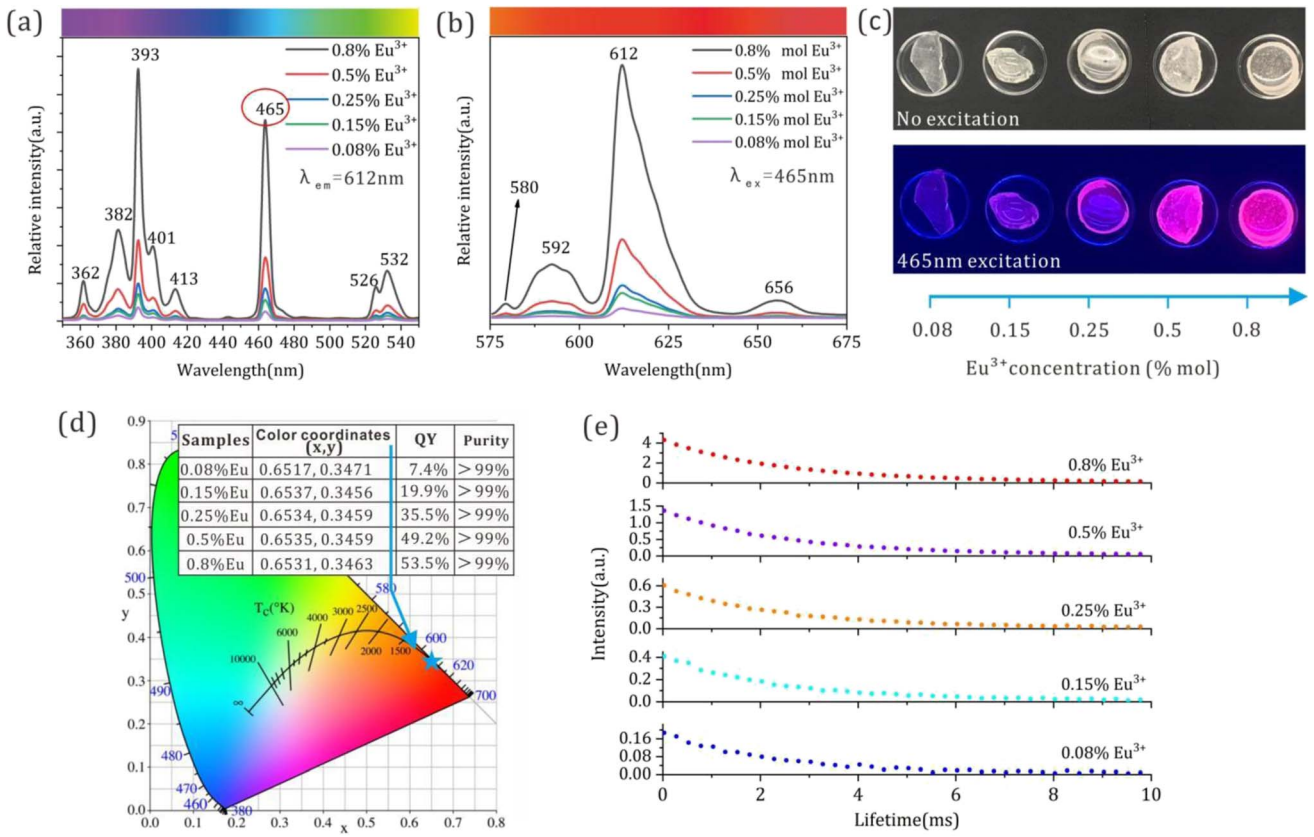

Fig. 3 (a) and (b) Excitation and emission spectra; (c) and (d) optical photos and CIE-1931 chromaticity coordinate diagram of the QDs under excitation of blue light with a wavelength of 465 nm, the corresponding optical parameters including CIE chromaticity coordinate diagram values, QY and color purity were inserted; (e) fluorescence decay curve.

of CdSe/CdS (see Fig. S4b†), all the residual peaks at 592, 612, and 656 nm originated from the electronic energy level transition of $^5D_0$–$^7F_1$, $^5D_0$–$^7F_2$, and $^5D_0$–$^7F_3$ from Eu^{3+}.[29] With the variation in Eu^{3+} ion concentrations from 0.08% to 0.8% mol, except for the enhancement of PL spectra intensity, the FWHM of the PL spectra, the position of the excitation, and emission peak have no variation, thereby indicating the luminescence color stability of the CdSe/CdS:Eu^{3+} inorganic QDs. The optical images and CIE chromaticity coordinate diagrams of the CdSe/CdS:Eu^{3+} inorganic QDs doped with various Eu^{3+} concentrations under the excitation of 465 nm in a dark environment were also presented in Fig. 3c and d to certify the enhanced red luminescence, high transparency and color stability of the CdSe/CdS:Eu^{3+} QDs. From the PL emission spectra and optical images, it can be concluded that the increasing Eu^{3+} concentration in the range of 0.08–0.8% contributes to improving the red emission of the inorganic CdSe/CdS:Eu^{3+} QDs. Moreover, the detailed CIE chromaticity coordinate values and QY, and color purity of the QDs samples, are inserted in Fig. 3d. All inorganic QD samples showed more than 99% color purity, and the QY also increased rapidly from 7.4% to 53.5% when the Eu^{3+} concentration increased to 0.8%, thereby suggesting the great potential of the CdSe/CdS:Eu^{3+} inorganic QDs as color converters for wLED. Additionally, the PL emission spectra, optical photos, quantum yield (QY), and CIE chromaticity coordinates at 30 days and 60 days supplied in Fig. S7 and Table S1† certified the long-term optical stability of the inorganic CdSe/CdS:Eu^{3+} QDs.

Fig. 3e presents the fluorescence lifetime decay curve of the CdSe/CdS:Eu^{3+} QDs. In detail, the fluorescence lifetime decay curves agree with the following double exponential equations *via* Gaussian fitting:[30]

$$I = A_1 \exp\left(\frac{-t}{\tau_1}\right) + A_2 \exp\left(\frac{-t}{\tau_2}\right) + R, \quad (1)$$

$$A_1 = \tau_1/(\tau_1 + \tau_2), \quad (2)$$

$$A_2 = \tau_2/(\tau_1 + \tau_2), \quad (3)$$

where I represents the integral area of the PL emission spectrum, t is the time, A_1 and A_2 are the fitting constants, τ_1 and τ_2 are the fast and slow decay lifetimes, respectively, and R is the correction coefficient. The average fluorescence lifetime of CdSe/CdS:Eu^{3+} QDs can be calculated using the following formula:

$$T = \left(A_1\tau_1^2 + A_2\tau_2^2\right)/\left(A_1\tau_1 + A_2\tau_2\right). \quad (4)$$

Compared with the CdSe/CdS QDs,[31] the fluorescence lifetime of the CdSe/CdS:Eu^{3+} inorganic QDs was prolonged significantly from nanosecond to millisecond level. Moreover, the increased Eu^{3+} concentration in the range of 0.08–0.5% contributes to prolonging the fluorescence lifetime of the QD samples from 5.91 ms to 8.05 ms, accompanied by the increase in PLQY. This suggests that the doped Eu^{3+} ions entered the lattice of CdSe/CdS QDs and improved the interface defects between the QDs and glass matrix, and this contributed to eliminating the non-radiative transition paths to increase the fluorescence lifetime of inorganic QDs. However, by continuously increasing Eu^{3+} concentration to 0.8%, the fluorescence lifetime decreased to 7.83 ms owing to the concentration quenching effect.[32] The unified double exponential behavior of the fluorescence lifetime decay curve suggested that the inorganic CdSe/CdS QDs matrix provided a homogenous electronic transition environment for Eu^{3+} ions and certified that Eu^{3+} ions were incorporated into the CdSe/CdS QDs lattice.

To explore the reason for the contribution of Eu^{3+} ions to the enhanced red emission of CdSe/CdS QDs, the absorption spectra of the CdSe/CdS:Eu^{3+} QDs are illustrated in Fig. 4. The absorption spectra of the CdSe/CdS:Eu^{3+} QDs displayed strong absorption from UV to visible light in the range of 350–550 nm with characteristic absorption peaks at 393, 465, 526 and 532 nm, which agrees with the excitation spectra. Except for the absorption peak of 393 nm belonging to CdSe/CdS, the residual characteristic absorption peaks must be assigned to the absorption of Eu^{3+}, demonstrating that some kinds of energy upconversion may happen from CdSe/CdS to Eu^{3+}, which leads to an improvement in red emission. Furthermore, in comparison with the PL emission and absorption spectra of CdSe/CdS:Eu^{3+} QDs, no overlap area can be observed, indicating that there is no energy re-absorption in the CdSe/CdS:Eu^{3+} QD system, which avoided lots of energy loss. This is another reason for the enhanced red emission of CdSe/CdS:Eu^{3+} QDs.

Consequently, a possible luminescence mechanism of the inorganic CdSe/CdS:Eu^{3+} QDs is depicted in Fig. 4f. The free electrons in the valence band jump to the conduction band under the excitation of a blue light source and then return to the valence band immediately and combine with the electron hole to release the luminescence of CdSe/CdS QDs with a wavelength of 580 nm. Additionally, a luminescence energy transfer occurred from CdSe/CdS QDs to the incorporated Eu^{3+} ions, where the free electrons of Eu^{3+} ions could be stimulated to jump to an energy level of $^5D_0$ from $^7F_0$. Notably, the excited state electrons of Eu^{3+} show a special energy up-conversion process, which can jump to higher energy levels of $^5D_1$, $^5D_2$, and $^5D_3$, and then release enhanced red luminescence with wavelengths of 595, 612, and 656 nm when returning from the states of $^7F_1$, $^7F_2$ and $^7F_3$, corresponding to its electronic energy level transitions of $^5D_0$–$^7F_1$, $^5D_0$–$^7F_2$, and $^5D_0$–$^7F_3$, respectively.

To further investigate the application feasibility of the prepared red emitting all-inorganic CdSe/CdS:Eu^{3+} QDs in wLED, the EL spectra of the wLED devices were measured by coupling the InGaN blue LED chip (EL spectra were supplied in Fig. S5a†) with G2762 green phosphors (PL spectra were supplied in Fig. S5b†) and CdSe/CdS:Eu^{3+} inorganic QDs (Fig. 5). To construct the wLED, the CdSe/CdS:Eu^{3+} inorganic QDs are pulverized into glass powders and combined with Intematix G2762 green phosphors to create a composite glass plate with a thickness of 0.25 mm. Subsequently, the composite glass plate is mounted on the InGaN blue LED chip under an operating current of 20 mA. Based on the QY and optical performance of the CdSe/CdS:Eu^{3+} QDs, two kinds of wLEDs were fabricated by selecting CdSe/CdS:0.5%Eu^{3+} and CdSe/

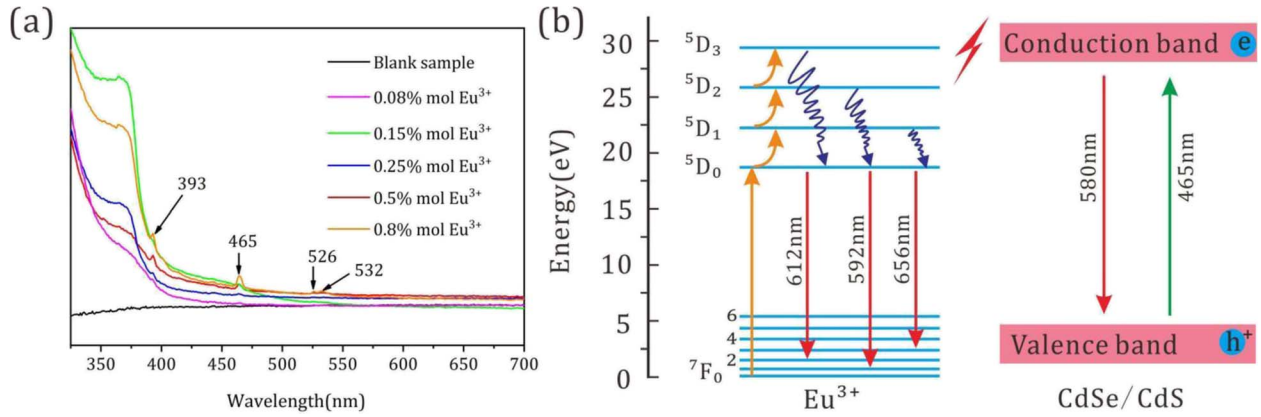

Fig. 4 (a) Absorption spectra of CdSe/CdS:Eu^{3+} QD. (b) Energy level diagram of CdSe/CdS:Eu^{3+} QD glass and possible photoluminescence energy transfer mechanism.

CdS:0.8%Eu^{3+} QDs as color converters. As depicted in Fig. 5a and b, stable blue/green/red emissions can be detected in the EL spectra. Pure white light and warm white light were produced by yielding white light with tunable CCT (5333 K and 5217 K), CRI (92.1 and 89.5), and LE (88.3 and 91.1 lm W^{-1}) (Fig. 5c and insets of Fig. 5a and b). Obviously, the warm white light of the wLED originated from the increasing red component of the EL spectra. Furthermore, the increase in Eu^{3+} ions doped into inorganic CdSe/CdS QDs contributes to improved LE, which is comparable to those devices based on inorganic halide perovskite $CsPbI_2$/P-Y_2O_3 (61 lm W^{-1}),[33] colloidal $CsPbBr_1I_2$-TS-1 QDs and YAG:Ce^{3+} phosphor (95 lm W^{-1}),[34] Gd-doped $CsPbBrI_2$ nanocrystals (90.09 lm W^{-1}),[35] and $CaAlSiN_3$:-Eu^{2+} phosphors glass (90.3 lm W^{-1})[36] reported in the literature. Furthermore, the high LE value is not based on the sacrifice of the color rendering index, which is quite different from those of previously reported studies, where the increase in CRI decreases LE.[37,38] This may be attributed to the luminescence energy transfer of CdSe/CdS-Eu^{3+} and the high transmittance of the inorganic CdSe/CdS:Eu^{3+} QDs.[39,40] The overlap area between the

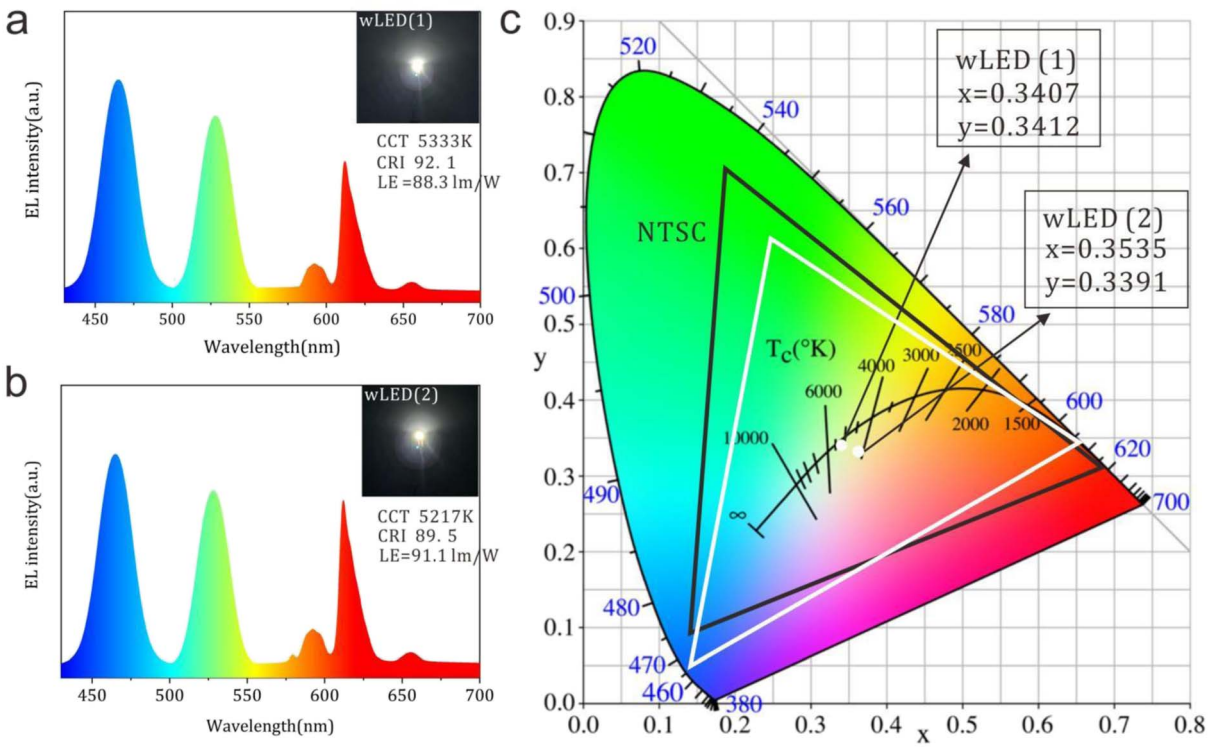

Fig. 5 (a) and (b) EL spectra of the self-assembled wLED devices by coupling GaN blue chip with G2762 green phosphors and the prepared inorganic CdSe/CdS:0.5%Eu^{3+} QDs and CdSe/CdS:0.8%Eu^{3+} QDs; (c) CIE-1931 chromaticity coordinate diagram of the as-prepared LED device; inset: the corresponding optical images of the wLED devices driven by a 20 mA operation current.

excitation spectrum of the green phosphor and the PL emission spectrum of the CdSe/CdS:Eu^{3+} QDs in Fig. S5b–d† indicated that the luminescence of green phosphor could be absorbed by the inorganic QDs to reduce energy loss, and this is also another reason for the excellent LE performance of the wLED device. In comparison with the National Television Standards Committee (NTSC) color gamut (black line in Fig. 5c), 91% of the NTSC color gamut (white line) could be obtained by calculating the CIE-1931 area that comprises the chromaticity coordinate of the blue InGaN LED chip, G2762 green phosphor, and red inorganic CdSe/CdS:0.5%Eu^{3+} QDs, thereby demonstrating the excellent color reproduction of the inorganic CdSe/CdS:Eu^{3+} QDs and great potential in wLED and other optical display devices.

Conclusion

Herein, we successfully fabricated a complete inorganic red emitting QD CdSe/CdS:Eu^{3+} with high transmittance and efficient quantum efficiency, as well as long-term stable optical performance, by incorporating Eu^{3+} ions into silicate glass-based CdSe/CdS QDs using a facile one-step melt quenching method. Enhanced red luminescence could be observed by increasing Eu^{3+} concentration under the excitation of 465 nm, and up to 53.5% of quantum yield was achieved when Eu^{3+} mole concentration increased to 0.8%. The improvement in the red luminescence was attributed to the energy transfer of CdSe/CdS-Eu^{3+} and energy up-conversion of Eu^{3+} in the electronic energy level transitions of $5D_0$–$7F_1$, $5D_0$–$7F_2$, and $5D_0$–$7F_3$. A warm white light (CCT = 5217 K) with 89.5 of CRI and 91.1 lm W^{-1} of LE was obtained by mounting the as-prepared CdSe/CdS:0.8% Eu^{3+} inorganic QDs and commercial Intematix G2762 green phosphor on the InGaN blue LED chip, which is comparable to those of phosphor- and CQD-based wLEDs. Furthermore, 91% of the NTSC color gamut was obtained, demonstrating the excellent color reproduction of the inorganic CdSe/CdS:Eu^{3+} inorganic QDs and great potential as color converters for wLED and LED displays.

Conflicts of interest

There are no conflicts to declare.

Acknowledgements

This work was financially supported by the Natural Science Foundation of Fujian Province (No. 2020J05173), Major Science and Technology Project of Fuzhou city (No. 2021-ZD-298) and Major Science and Technology Project of Jiebang Guashuai of Fuzhou city (No. 2022-ZD-007).

References

1 R. Wang, M. Y. Wang, G. Li, J. H. Zhang, Y. J. Zhang, H. Lin, E. Y. B. Pun and D. S. Li, Red-emitting improvement of $CaAlSiN_3$:Eu^{2+} phosphor-in-glass: Insight into the effect of atmospheric pressure preparation on photoluminescence properties and thermal degradation, *J. Lumin.*, 2020, **225**, 117390.

2 Y. H. Nam, W. J. Chung and W. B. Im, Phosphor in glass using β-SiAlON:Eu^{2+}, $CaAlSiN_3$:Eu^{2+} and Nd-doped silicate glass for enhanced color gamut of white LED, *J. Alloy Compd.*, 2021, **851**, 156945.

3 P. Dang, G. Li, X. Yun, Q. Zhang, D. Liu, H. Lian, M. Shang and J. Lin, Thermally stable and highly efficient red-emitting Eu^{3+}-doped $Cs_3GdGe_3O_9$ phosphors for WLEDs: non-concentration quenching and negative thermal expansion, *Light: Sci. Appl.*, 2021, **10**, 29.

4 J. S. Li, Y. Tang, Z. T. Li, J. X. Li, X. R. Ding, B. H. Yu, S. D. Yu, J. Z. Ou and H. C. Kuo, Toward 200 Lumens per Watt of Quantum-Dot White-Light-Emitting Diodes by Reducing Reabsorption Loss, *ACS Nano*, 2021, **15**, 550–562.

5 X. Li, W. Cai, H. Guan, S. Zhao, S. Cao, C. Chen, M. Liu and Z. Zang, Highly stable $CsPbBr_3$ quantum dots by silica-coating and ligand modification for white light-emitting diodes and visible light communication, *Chem. Eng. J.*, 2021, **419**, 129551.

6 L. Rao, Q. Zhang, M. Wen, Z. Mao, H. Wei, H. Chang and X. Niu, Solvent regulation synthesis of single-component white emission carbon quantum dots for white light-emitting diodes, *Nanotechnol. Rev.*, 2021, **10**, 465–477.

7 Z. Li, C. Song, J. Li, G. Liang, L. Rao, S. Yu, X. Ding, Y. Tang, B. Yu, J. Ou, U. Lemmer and G. Gomard, Highly Efficient and Water-Stable Lead Halide Perovskite Quantum Dots Using Superhydrophobic Aerogel Inorganic Matrix for White Light-Emitting Diodes, *Adv. Mater. Technol.*, 2020, 1900941.

8 X. Yang, Z. Zhang, T. Ding, N. Wang, G. Chen, C. Dang, H. V. Demir and X. Sun, High-efficiency all-inorganic full-colour quantum dot light-emitting diodes, *Nano energy*, 2018, **46**, 229–233.

9 Q. Xu, X. Li, Q. Lin, H. Shen, H. Wang and Z. Du, Improved Efficiency of All-Inorganic Quantum-Dot Light-Emitting Diodes via Interface Engineering, *Front. Chem.*, 2020, **8**, 265.

10 M. Xia, J. Luo, C. Chen, H. Liu and J. Tang, Semiconductor quantum dots-embedded inorganic glasses: fabrication, luminescent properties, and potential applications, *Adv. Opt. Mater.*, 2019, 7(21), 1900851.

11 Y. Tong, Q. Wang, X. Liu, E. Mei, X. Liang and W. Xiang, The promotion of TiO2 induction for finely tunable self-crystallized $CsPbX_3$ (X = Cl, Br and I) nanocrystal glasses for LED backlighting display, *Chem. Eng. J.*, 2022, **429**, 132391.

12 Y. Wang, F. Yuan, Y. Dong, J. Li, A. Johnston, B. Chen, M. I. Saidaminov, C. Zhou, X. Zheng, Y. Hou, K. Bertens, H. Ebe, D. Ma, Z. Deng, S. Yuan, R. Chen, L. K. Sagar, J. Liu, J. Fan, P. Li, X. Li, Y. Gao, M. K. Fung, Z. H. Lu, O. M. Bakr and L. Liao, All-Inorganic Quantum-Dot LEDs Based on a Phase-Stabilized α-CsPbI3 Perovskite, *Angew. Chem., Int. Ed.*, 2021, **60**, 16164.

13 H. Zhang, M. Jin, X. Liu, Y. Zhang, Y. Yu, X. Liang, W. Xiang and T. Wang, The preparation and up-conversion properties of full spectrum $CsPbX_3$ (X = Cl, Br, I) quantum dot glasses, *Nanoscale*, 2019, **11**, 18009.

14 C. Chen, L. Nie, Y. Huang, S. Xi, X. Liu, X. Zhang, T. Shi, G. Liao, S. Liu and Z. Tang, Embedded growth of colorful $CsPbX_3$ (X = Cl, Br, I) nanocrystals in metal-organic frameworks at Room Temperature, *Nanotechnology*, 2022, **33**, 175603.

15 D. Chen, Y. Liu, C. Yang, J. Zhong, S. Zhou, J. Chen and H. Huang, Promoting photoluminescence quantum yields of glass-stabilized $CsPbX_3$ (X=Cl, Br, I) perovskite quantum dots through fluorine doping, *Nanoscale*, 2019, **11**, 17216.

16 B. Shu, Y. Chang, J. Zhang, X. Cheng and D. Yu, Synthesis and photoluminescence kinetics of Ce^{3+}-doped $CsPbI_3$ QDs with near-unity PLQY, *Nano Res.*, 2021, **14**(10), 3352–3357.

17 A. Swarnkar, W. J. Mir and A. Nag, Can B–site doping or alloying improve thermal- and phase-stability of all-inorganic $CsPbX_3$ (X = Cl, Br, I) perovskites?, *ACS Energy Lett.*, 2018, **3**, 286.

18 S. Seth, T. Ahmed, A. De and A. Samanta, Tackling the defects, stability, and photoluminescence of $CsPbX_3$ perovskite nanocrystals, *ACS Energy Lett.*, 2019, **4**, 1610.

19 C. H. Bi, S. V. Kershaw, A. L. Rogach and J. J. Tian, Improved stability and photodetector performance of $CsPbI_3$ perovskite quantum dots by ligand exchange with aminoethanethiol, *Adv. Funct. Mater.*, 2019, **29**, 1902446.

20 P. Liu, Y. Lou, S. Ding, W. Zhang, Z. Wu, H. Yang, B. Xu, K. Wang and X. Sun, Green InP/ZnSeS/ZnS Core Multi-Shelled Quantum Dots Synthesized with Aminophosphine for Effective Display Applications, *Adv. Funct. Mater.*, 2021, **31**, 2008453.

21 B. B. Jin, S. Y. Kong, G. Q. Zhang, X. Q. Chen, H. S. Ni, F. Zhang, D. J. Wang and J. H. Zeng, Voltage-assisted SILAR deposition of CdSe quantum dots to construct a high performance of ZnS/CdSe/ZnS quantum dot-sensitized solar cells, *J. Colloid Interf. Sci.*, 2021, **586**, 640.

22 W. Li, K. Li, X. Zhao, C. Liu and F. X. Coudert, Defective Nature of CdSe Quantum Dots Embedded in Inorganic Matrices, *J. Am. Chem. Soc.*, 2022, **144**(25), 11296–11305.

23 U. Latief, S. U. Islam, Z. Khan and M. S. Khan, Luminescent Manganese/Europium doped ZnS quantum dots: Tunable emission and their application as fluorescent sensor, *J. Alloy Compd.*, 2022, **910**, 164889.

24 C. Lu, Y. Duan, P. Li, Y. Lu, S. Xu and J. Zhang, Polychromatic tunable luminescence of Eu^{3+} doped $CsPbBr_3$ quantum dot glass ceramic induced by mechanical crystallization, *Ceram. Int.*, 2022, **48**, 13826.

25 E. Erdinç, V. Naji, U. Ekim, U. Nazlıcan, Ç. E. Miray and E. E. Ali, Ultra-stable Eu^{3+}/Dy^{3+} co-doped $CsPbBr_3$ quantum dot glass nanocomposites with tunable luminescence properties for phosphor-free WLED applications, *J. Alloy Compd.*, 2022, **909**, 164650.

26 X. Jing, D. Zhou, R. Sun, Y. Zhang, Y. n Li, X. Li, Q. n Li, H. Song and B. Liu, Enhanced Photoluminescence and Photoresponsiveness of Eu^{3+} Ions-Doped $CsPbCl_3$ Perovskite Quantum Dots under High Pressure, *Adv. Funct. Mater.*, 2021, **31**, 2100930.

27 K. Han, W. B. Im, J. Heo and W. J. Chung, A complete inorganic colour converter based on quantum-dot-embedded silicate glasses for white light-emitting-diodes, *Chem. Commun.*, 2016, **52**, 3564.

28 K. Han, W. B. Im, J. Heo and W. J. Chung, Compositional dependency of Cd-S-Se quantum dots within silicate glass on color conversion for a white LED, *J. Am. Ceram. Soc.*, 2019, **102**, 1703.

29 R. Yuan, J. Liu, H. Zhang, Z. Zhang, G. Shao, X. Liang and W. Xiang, Eu^{3+}-doped $CsPbBr_{1.5}I_{1.5}$ quantum dots glasses: A strong competitor among red fluorescence solid materials, *J. Am. Ceram. Soc.*, 2018, **101**, 4927.

30 P. P. Li, Y. Lu, Y. M. Duan, S. Q. Xu and J. J. Zhang, Potential application of perovskite glass material in photocatalysis field, *J. Phys. Chem. C*, 2021, **125**, 2382.

31 P. Sara, D. Dirk, F. Sebastian, F. Axel, W. Andreas and C. B. Nadja, Aerogels from CdSe/CdS Nanorods with Ultra-long Exciton Lifetimes and High Fluorescence Quantum Yields, *Adv. Mater.*, 2015, **27**, 6152.

32 J. Sun, W. Zheng, P. Huang, M. Zhang, W. Zhang, Z. Deng, S. Yu, M. Jin and X. Chen, Efficient Near-Infrared Luminescence in Lanthanide-Doped Vacancy-Ordered Double Perovskite Cs_2ZrCl_6 Phosphors via Te^{4+} Sensitization, *Angew. Chem., Int. Ed.*, 2022, **61**, e202201993.

33 X. Li, Y. Wei, P. Dang, X. Xiao, H. Xiao, G. Zhang, G. Li and J. Lin, Enhancing the stability of perovskite quantum dots $CsPbX_3$ (X=Cl, Br, I) by encapsulation in porous Y_2O_3 nanoparticles for WLED applications, *Mater. Res. Bull.*, 2022, **146**, 111592.

34 J. Li, Z. Chen, J. Liu, E. Mei, X. Liang, J. Liu and W. Xiang, Novel and stable $CsPbX_3$-TS-1 (X= Br, I) nanocomposites for light-emitting diodes, *Chem. Eng. J.*, 2021, **426**, 131327.

35 Q. He, Y. Zhang, Y. Yu, Y. Chen, M. Jin, E. Mei, X. Liang, L. Zhai and W. Xiang, Ultrastable Gd^{3+} doped $CsPbBrI_2$ nanocrystals red glass for high efficiency WLEDs, *Chem. Eng. J.*, 2021, **411**, 128530.

36 Y. Zhang, Z. Zhang, X. Liu, G. Shao, L. Shen, J. Liu, W. Xiang and X. Liang, A high quantum efficiency CaAlSiN3:Eu^{2+} phosphor-in-glass with excellent optical performance for white light-emitting diodes and blue laser diodes, *Chem. Eng. J.*, 2020, **401**, 125983.

37 T. Deng, E. Song, Y. Zhou and J. Yuan, Implementation of high color quality, high luminous warm WLED using efficient and thermally stable Rb_3AlF_6:Mn^{4+} as red color converter, *J. Alloy Compd.*, 2019, **795**, 453.

38 X. Liu, X. Qian, P. Zheng, X. Chen, Y. Feng, Y. Shi, J. Zou, R. Xie and J. Li, Composition and structure design of three-layered composite phosphors for high color rendering chip-on-board light-emitting diode devices, *J. Adv. Ceram.*, 2021, **10**(4), 729–740.

39 Z. Yang, L. Zhao, M. Li, Q. Yang, Z. Fang, L. Yang, X. Yu, J. Qiu, Y. Yang and X. Xu, Perovskite quantum dots growth in situ in transparent medium for short wavelength shielding, *J. Am. Ceram. Soc.*, 2020, **103**, 4150.

40 P. M. Tan, N. X. Ca, N. T. Hien, H. T. Van, P. V. Do, L. D. Thanh, V. H. Yen, V. P. Tuyen, Y. Peng and P. T. Tho, New insights on the energy transfer mechanisms of Eu-doped CdS quantum dots, *Phys. Chem. Chem. Phys.*, 2020, **22**, 6266.

